Stefan Krone

# Wireless Communications with Coarse Quantization: Information-Theoretic Analysis and System Design Aspects

Beiträge aus der Informationstechnik

Mobile Nachrichtenübertragung
Nr. 58

**Stefan Krone**

# Wireless Communications with Coarse Quantization: Information-Theoretic Analysis and System Design Aspects

VOGT

Dresden 2012

Bibliografische Information der Deutschen Bibliothek
Die Deutsche Bibliothek verzeichnet diese Publikation in der Deutschen Nationalbibliografie; detaillierte bibliografische Daten sind im Internet über http://dnb.ddb.de abrufbar.

Bibliographic Information published by the Deutsche Bibliothek
The Deutsche Bibliothek lists this publication in the Deutsche Nationalbibliografie; detailed bibiograpic data is available in the internet at http://dnb.ddb.de.

Zugl.: Dresden, Techn. Univ., Diss., 2012

Die vorliegende Arbeit stimmt mit dem Original der Dissertation „Wireless Communications with Coarse Quantization: Information-Theoretic Analysis and System Design Aspects“ von Stefan Krone überein.



Gesetzt vom Autor

ISBN 978-3-938860-51-9

Jörg Vogt Verlag
Niederwaldstr. 36
01277 Dresden
Germany

Phone: +49-(0)351-31403921
Telefax: +49-(0)351-31403918
e-mail: info@vogtverlag.de
Internet : www.vogtverlag.de

TECHNISCHE UNIVERSITÄT DRESDEN

# Wireless Communications with Coarse Quantization: Information-Theoretic Analysis and System Design Aspects

**Stefan Krone**

von der Fakultät Elektrotechnik und Informationstechnik
der Technischen Universität Dresden

zur Erlangung des akademischen Grades eines

**Doktoringenieurs**

(Dr.-Ing.)

genehmigte Dissertation

| | |
|---|---|
| Vorsitzender: | Prof. Dr.-Ing. Eduard A. Jorswieck |
| Gutachter: | Prof. Dr.-Ing. Gerhard P. Fettweis |
| | Prof. Dr. techn. Josef A. Nossek |

| | |
|---|---|
| Tag der Einreichung: | 06. Februar 2012 |
| Tag der Verteidigung: | 20. April 2012 |

# Abstract

Wireless communications systems have seen enormous advancements over the last decades and have emerged as an integral part of everyday's life. This great success creates ever more ambitious applications such as wideband radio links in computer racks or wide area sensor networks with devices that shall consume almost no energy. Applications like these impose serious challenges on the required hardware, which is calling for new system design paradigms. One of the most serious hardware issues is the data conversion at the transmitter and receiver. It is restricted to coarse quantization when large sampling rates and/or minimum energy consumption shall be achieved. New system concepts have to account for this limitation, which necessitates a fundamental understanding of theoretical performance limits and corresponding system design aspects. This thesis analyzes these aspects from an information-theoretic perspective.

The analysis builds on a general model of wireless communications systems with limited data conversion. The model is simplified throughout the thesis to deduce channel models that can be treated analytically, e.g., to calculate the channel capacity with coarse quantization at the receiver. Common data converter architectures are reviewed, and their technological limitations are discussed. It is shown that large sampling rates and coarse quantization are reasonable and most energy-efficient for future system designs. Concepts for optimizing a given quantization characteristic are derived and compared. The results indicate that an amplitude distortion perspective is not appropriate to address the maximum data rate of a system when the quantization resolution is low. The metric to be considered for the optimization is the mutual information. Using this metric, it is shown for conventional modulation schemes and additive white Gaussian noise channels that the quantization resolution at the receiver can be kept sufficiently small without degrading the maximum data rate. More fundamentally, the capacity and capacity-achieving transmit schemes are studied for different types of wireless channels with coarse quantization at the receiver. The Cutting Plane algorithm is used to calculate the capacity of additive white Gaussian noise channels with coarse quantization. A closed-form capacity expression is derived for the special case of 1-bit quantization. Capacity lower bounds are discussed for time dispersive channels, because an exact capacity calculation is rather impossible. Frequency-flat fading channels are considered for the case of 1-bit quantization, which yields closed-form solutions for the ergodic channel capacity and the optimal outage behavior. Furthermore, oversampling is considered together with 1-bit quantization. It is shown that additive noise and inter-symbol-interference can improve the channel capacity with oversampling as they increase the effective quantization resolution to more than 1 bit. This effect results from stochastic resonance and may have a significant impact on future system designs. The last part of the thesis derives linear channel (pre-)equalization schemes that incorporate the data conversion at the transmitter and receiver. It is shown, that fractionally-spaced (pre-)equalization, which builds on oversampling, can be conveniently combined with time-interleaved data converter architectures.

In general, it is found that coarse quantization may not be a drawback but an important enabler for emerging wireless applications.

# Zusammenfassung

Drahtlose Kommunikationssysteme haben in den letzten Jahrzehnten große Fortschritte erfahren und sind Bestandteil des Alltags geworden. Dieser Erfolg antizipiert immer herausfordernde Anwendungen, so zum Beispiel breitbandige Funkverbindungen in Computerracks und drahtlose Sensornetzwerke mit Sensoren, die minimale Energie verbrauchen. Solche Anwendungen stellen höchste Hardwareanforderungen, die nur mit neuen Systementwurfsparadigmen realisierbar sind. Eines der größten Probleme ist die Datenwandlung am Sender und Empfänger. Sie ist auf geringe Quantisierung beschränkt, wenn hohe Samplingraten und / oder minimaler Energieverbrauch erreicht werden sollen. Neuartige Systemkonzepte müssen dies berücksichtigen. Dafür müssen die theoretischen Grenzen der Systemleistungsfähigkeit und geeignete Entwurfsaspekte bekannt sein. Die vorliegende Arbeit widmet sich diesen Punkten aus informationstheoretischer Sicht.

Der Analyse liegt ein allgemeines Modell für Kommunikationssysteme mit limitierter Datenwandlung zu Grunde. Dieses wird vereinfacht, um Kanalmodelle abzuleiten, die analytisch untersucht werden können, um beispielsweise die Kanalkapazität mit Quantisierung am Empfänger zu berechnen. Übliche Datenwandlerarchitekturen werden betrachtet und die technologischen Grenzen diskutiert. Es wird gezeigt, dass hohe Samplingraten und grobe Quantisierung sehr sinnvoll und energieeffizient für zukünftige Systementwürfe sind. Konzepte zur Optimierung gegebener Quantisierungscharakteristiken werden hergeleitet und verglichen. Die Ergebnisse zeigen, dass sich eine Betrachtung der Amplitudenverzerrung nicht eignet, um die maximale Datenrate von System zu bestimmen, wenn die Quantisierungsauflösung gering ist. Die für die Optimierung notwendige Metrik ist die Transinformation. Unter Verwendung dieser Metrik wird für konventionelle Modulationsverfahren und Kanäle mit additivem weißen Gaußschen Rauschen gezeigt, dass die Quantisierungsauflösung am Empfänger gering sein kann, ohne die maximale Datenrate zu beeinträchtigen. Noch grundlegender werden die Kapazität und kapazitätserreichende Sendeschemata für verschiedene Funkkanäle mit grober Quantisierung am Empfänger untersucht. Der Cutting-Plane-Algorithmus wird zur Berechnung der Kapazität von Kanälen mit additivem weißen Gaußschen Rauschen und grober Quantisierung verwendet. Ein geschlossener Kapazitätsausdruck wird für 1-Bit Quantisierung hergeleitet. Für zeitdispersive Kanäle werden untere Kapazitätsgrenzen diskutiert, da eine exakte Berechnung schwierig ist. Frequenzflache Schwundkanäle werden für den Fall von 1-Bit Quantisierung betrachtet. Dies liefert geschlossene Lösungen für die ergodische Kapazität und optimales Ausfallverhalten. Zudem wird 1-Bit Quantisierung in Verbindung mit Überabtastung untersucht. Es zeigt sich, dass Rauschen und Intersymbolinterferenz die Kapazität mit Überabtastung erhöhen, da sie die effektive Quantisierungsauflösung auf über 1 Bit steigern. Dies beruht auf stochastischer Resonanz und kann neuartige Systemkonzepte ermöglichen. Der letzte Abschnitt der Arbeit leitet lineare Kanalentzerrungsschemata her, welche die Datenwandlung an Sender und Empfänger einbeziehen. Es wird gezeigt, dass sich eine Kanalentzerrung mit Überabtastung geeignet mit zeitverschachtelten Datenwandlerarchitekturen kombinieren lässt.

Insgesamt zeigt die Arbeit auf, dass grobe Quantisierung kein Nachteil sein muss, sondern neuartige Anwendungen der drahtlosen Kommunikation erst ermöglicht.

# Acknowledgments

This thesis is the result of my work at the Vodafone Chair Mobile Communications Systems at Technische Universität Dresden. I owe my sincere gratitude to Prof. Gerhard P. Fettweis for his guidance and continued support during the last years. I am indebted to him not only for providing me with one of the most exciting research topics I could have thought of, but also for putting his trust in me when I took over responsibility in the research project EASY-A and when he asked me to become a group leader in his team. It was also he who enabled an inspiring research visit to the University of California in Santa Barbara. All of this allowed me to develop my academic and personal skills. I am also grateful to Prof. Joseph A. Nossek for serving as a second referee for this thesis.

Parts of this thesis would not exist without the support of Prof. Upamanyu Madhow and his group at the University of California in Santa Barbara. In particular, I would like to acknowledge the valuable exchange of ideas with Jaspreet Singh and Sriram Venkateswaran. I am also thankful to the German Academic Exchange Service (DAAD) for providing financial support for this research visit. Moreover, I would like to thank Michael Joham and Behnam Sedighi for sharing their expertise with me. Many thanks go also to Surbhi Maheshwari for her survey on modern data converters.

I am very grateful to all my colleagues and friends at the Vodafone Chair who have supported this thesis with their expertise and who have made every day in the office an enjoyable day. In particular, I would like to share the credit of this thesis with Eckhard Ohlmer and Peter Rost, who have shaped this work with their advices and through a frequent exchange of ideas. I am indebted to Michael Lentmaier and Ines Riedel for taking their time to proof-read parts of the manuscript. I also offer my regards to Ernesto Zimmermann, who has been an excellent mentor when I was a freshman at the Vodafone Chair. Finally, I would like to thank Falko Guderian, Hermann Hensel, Björn Almeroth, Marco Krondorf and Steffen Bitter for their commitment to hardware, which let our vision of a working 60 GHz link become reality in the EASY-A project. I appreciate the project funding provided by the German Federal Ministry of Education and Research, which has been the financial basis for major parts of the research carried out for this thesis. I will also retain fond memories of the fruitful cooperation with all project partners.

Last but not least, I thank all my close friends who have never stopped reminding me that there is life outside the office. The great time outdoors has helped a lot to refresh and keep sight of the goal. Still, this thesis would have remained a dream without my family. I am deeply grateful for their patience and everlasting support which allowed me to master every challenge I met. The development of this thesis has taught me an important lesson that may be best expressed in the words of Jim Watkins: "A river cuts through rock, not because of its power, but because of its persistence."

# Contents

**Abstract / Zusammenfassung** **i**

**Acknowledgments** **iii**

**Contents** **v**

**Abbreviations** **ix**

**Nomenclature** **xi**

**1 Introduction** **1**
1.1 Wireless Data Transmission . . . . . 1
1.2 Data Conversion Bottleneck . . . . . 2
1.3 Outline of the Thesis . . . . . 3

**2 Fundamentals of Data Transmission** **5**
2.1 Objectives and Literature . . . . . 5
2.2 Signals in Communications . . . . . 6
2.2.1 Signal Types . . . . . 6
2.2.2 Data Conversion . . . . . 7
2.3 Wireless Communications Systems . . . . . 9
2.3.1 System Architecture . . . . . 10
2.3.2 Discrete Time Channel Model . . . . . 10
2.4 Mutual Information and Channel Capacity . . . . . 14
2.4.1 Mutual Information . . . . . 14
2.4.2 Channel Capacity and Optimal Inputs . . . . . 16
2.5 Summary . . . . . 18

**3 Technological and Physical Limits to Digital Signals** **19**
3.1 Objectives, Literature and Contributions . . . . . 19
3.2 State-of-the-Art Data Converters . . . . . 21
3.2.1 Principles and Architectures . . . . . 21
3.2.2 Performance Trends . . . . . 27
3.3 Technological Limitations and Physical Bounds . . . . . 30
3.3.1 Minimum Power Dissipation of Data Converters . . . . . 30
3.3.2 Physical Bounds for Information Rates . . . . . 34
3.3.3 Discussion and Illustration . . . . . 37
3.4 Summary and Conclusions . . . . . 38

**4 Concepts for Optimized Quantization** **39**
4.1 Objectives, Literature and Contributions . . . 39
4.2 Preliminaries . . . 41
4.2.1 Classification of Optimization Metrics . . . 41
4.2.2 Adjusting Quantization Parameters . . . 42
4.3 Amplitude Distortion Perspective . . . 43
4.3.1 Mean Square Error . . . 43
4.3.2 Pseudo Quantization Noise . . . 45
4.4 Information-Theoretic Perspective . . . 49
4.4.1 Entropy and Mutual Information . . . 49
4.4.2 Rate Distortion Function . . . 52
4.5 Optimized Quantization of Distorted QAM Symbols . . . 53
4.5.1 Signal Model and Assumptions . . . 54
4.5.2 Minimum Mean Square Error . . . 56
4.5.3 Maximum Mutual Information . . . 59
4.5.4 Conclusions . . . 65
4.6 Summary . . . 65

**5 Capacity Analysis of Channels with Output Quantization** **67**
5.1 Objectives, Literature and Contributions . . . 67
5.2 General Bounds and Approximations . . . 70
5.2.1 Upper and Lower Bounds . . . 70
5.2.2 Capacity Approximations . . . 71
5.3 AWGN Channels with Output Quantization . . . 72
5.3.1 Discrete Time Channel Model . . . 73
5.3.2 Channel Capacity and Optimal Inputs . . . 74
5.3.3 Output versus Input Quantization . . . 85
5.3.4 Energy-Efficient ADC Parametrization . . . 86
5.3.5 Conclusions . . . 90
5.4 Time-Dispersive Channels with Output Quantization . . . 91
5.4.1 Discrete Time Channel Model . . . 91
5.4.2 Mutual Information and Optimal Inputs . . . 94
5.4.3 Lower Bounds of the Channel Capacity . . . 95
5.4.4 Two-Tap Channel with 1-Bit Output Quantization . . . 98
5.4.5 Conclusions . . . 103
5.5 Fading Channels with 1-Bit Output Quantization . . . 104
5.5.1 Discrete Time Channel Model and Fading Statistics . . . 104
5.5.2 Mutual Information for Instantaneous Fading States . . . 105
5.5.3 Ergodic Channel Capacity with Optimal Inputs . . . 107
5.5.4 Outage Probability Analysis . . . 110
5.5.5 Conclusions . . . 117
5.6 Summary . . . 117

**6 Prospects of 1-bit Quantization and Oversampling** **119**
6.1 Objectives, Literature and Contributions . . . 119
6.2 AWGN Channels with Rectangular Pulse Shapes . . . 121
6.2.1 Discrete Time System Model . . . 121
6.2.2 Sufficient Statistic . . . 123
6.2.3 Mutual Information with $L$-QAM . . . 124

6.2.4 Maximum Mutual Information at high SNR . . . . . . . . . . . . . . . . . . 127
6.2.5 Channel Capacity and Optimal Inputs . . . . . . . . . . . . . . . . . . . . . . 129
6.3 Numerical Analysis for Band-Limited AWGN Channels . . . . . . . . . . . . . . 137
6.3.1 Discrete Time System Model . . . . . . . . . . . . . . . . . . . . . . . . . . 137
6.3.2 Mutual Information Lower Bound . . . . . . . . . . . . . . . . . . . . . . . . 139
6.3.3 Numerical Evaluation . . . . . . . . . . . . . . . . . . . . . . . . . . . . . 142
6.4 Summary and Conclusions . . . . . . . . . . . . . . . . . . . . . . . . . . . . . . 144

**7 Linear Channel (Pre-)Equalization with Coarse Quantization 147**
7.1 Objectives, Literature and Contributions . . . . . . . . . . . . . . . . . . . . . . . 147
7.2 Fractionally-Spaced Equalization at the Receiver . . . . . . . . . . . . . . . . . . . 149
7.2.1 Discrete Time System Model . . . . . . . . . . . . . . . . . . . . . . . . . . 149
7.2.2 Equalizer Design and ADC Calibration . . . . . . . . . . . . . . . . . . . . . 153
7.2.3 Conceptual Summary . . . . . . . . . . . . . . . . . . . . . . . . . . . . . . 159
7.3 Fractionally-Spaced Pre-Equalization at the Transmitter . . . . . . . . . . . . . . 160
7.3.1 Discrete Time System Model . . . . . . . . . . . . . . . . . . . . . . . . . . 161
7.3.2 Pre-Equalizer Design and DAC Calibration . . . . . . . . . . . . . . . . . . 164
7.3.3 Conceptual Summary . . . . . . . . . . . . . . . . . . . . . . . . . . . . . . 170
7.4 Performance Evaluation and Interpretation . . . . . . . . . . . . . . . . . . . . . 171
7.4.1 System and Simulation Setup . . . . . . . . . . . . . . . . . . . . . . . . . 171
7.4.2 Equalization at the Receiver . . . . . . . . . . . . . . . . . . . . . . . . . . 172
7.4.3 Pre-Equalization at the Transmitter . . . . . . . . . . . . . . . . . . . . . . 175
7.5 Summary and Conclusions . . . . . . . . . . . . . . . . . . . . . . . . . . . . . . 177

**8 Summary and Future Work 179**
8.1 Overall Summary . . . . . . . . . . . . . . . . . . . . . . . . . . . . . . . . . . . 179
8.2 Topics for Future Work . . . . . . . . . . . . . . . . . . . . . . . . . . . . . . . . 181

**A 60 GHz Demonstrator for Multi-Gbps Wireless Data Links 183**
A.1 System Concept and Physical Layer Design . . . . . . . . . . . . . . . . . . . . . 183
A.2 Digital Baseband Implementation . . . . . . . . . . . . . . . . . . . . . . . . . . . 185
A.3 Demonstrator Integration . . . . . . . . . . . . . . . . . . . . . . . . . . . . . . . 187

**B Computation of Mutual Information and Channel Capacity 189**
B.1 Calculation of Mutual Information . . . . . . . . . . . . . . . . . . . . . . . . . . 189
B.1.1 Simulation-Based Approximation . . . . . . . . . . . . . . . . . . . . . . . . 189
B.1.2 Lower Bound for Discrete Channels with Memory . . . . . . . . . . . . . . . 190
B.2 Numerical Computation of the Channel Capacity . . . . . . . . . . . . . . . . . . 192
B.2.1 Blahut-Arimoto Algorithm . . . . . . . . . . . . . . . . . . . . . . . . . . . 193
B.2.2 Cutting-Plane Algorithm . . . . . . . . . . . . . . . . . . . . . . . . . . . . 194

**C Quantization Characteristics 197**
C.1 Maximum Entropy and MMSE Quantization of Gaussian Amplitudes (Tables) . 197
C.2 Uniform MMSE Quantization of Distorted QAM Symbols (Derivation) . . . . . . 200
C.3 ML Quantization of Distorted QAM Symbols (Derivation) . . . . . . . . . . . . . 202

**D Proofs of Theorems 205**
D.1 Theorem 2.1 . . . . . . . . . . . . . . . . . . . . . . . . . . . . . . . . . . . . . . 205
D.2 Theorems 5.1 to 5.8 . . . . . . . . . . . . . . . . . . . . . . . . . . . . . . . . . . 205
D.3 Theorem 6.1 . . . . . . . . . . . . . . . . . . . . . . . . . . . . . . . . . . . . . . 210

**List of Figures and Tables** **211**

**Bibliography** **214**

**Publications** **225**

**Curriculum Vitae** **229**

# Abbreviations

**Acronyms**

| | |
|---|---|
| AC | Alternating current. |
| ADC | Analog-to-digital converter. |
| AGC | Adaptive gain control. |
| ASK | Amplitude shift keying. |
| AWGN | Additive white Gaussian noise. |
| BER | Bit error rate. |
| BiCMOS | Bipolar CMOS. |
| BPSK | Binary phase shift keying. |
| CDF | Cumulative distribution function. |
| CSI | Channel state information. |
| CMOS | Complementary metal oxide semiconductor. |
| DAC | Digital-to-analog converter. |
| DBPSK | Differential binary phase shift keying. |
| DC | Direct current. |
| DMC | Discrete memoryless channel. |
| DQPSK | Differential quaternary phase shift keying. |
| FOM | Figure of merit. |
| FIR | Finite impulse response. |
| FPGA | Field programmable gate array. |
| GI | Guard interval. |
| IEEE | Institute of Electrical and Electronics Engineers. |
| IIR | Infinite impulse response. |
| ISI | Inter-symbol-interference. |
| ENOB | Effective number of bits. |
| ETUP | Energy-time uncertainty principle. |
| FIR | Finite impulse response. |
| i.i.d. | Independently identically distributed. |
| LOS | Line-of-sight. |
| ML | Maximum likelihood. |

| | |
|---|---|
| MSE | Mean square error. |
| MMSE | Minimum mean square error. |
| OSR | Oversampling ratio. |
| PAM | Pulse amplitude modulation. |
| PAPR | Peak-to-average power ratio. |
| PDF | Probability density function. |
| PMF | Probability mass function. |
| PQN | Pseudo quantization noise. |
| PSD | Power spectral density. |
| PSK | Phase shift keying. |
| QAM | Quadrature amplitude modulation. |
| QPSK | Quaternary phase shit keying. |
| RRC | Root-raised-cosine. |
| SAR | Successive approximation register. |
| SiGe | Silicon-Germanium. |
| SNR | Signal-to-noise ratio. |
| SQNR | Signal-to-quantization-noise ratio. |
| TI | Time-interleaved. |
| WF | Wiener filter. |
| ZF | Zero forcing. |

**Units of measure**

| | |
|---|---|
| % | Percent. |
| bpcu | Bits per channel use. |
| dB | Decibel. |
| dBm | Decibel (related to $10^{-3}$ W). |
| F | Farad. |
| Gbps | Gigabits per second ($10^9$ bits per second). |
| GHz | Gigahertz ($10^9$ Hertz). |
| J | Joule. |
| K | Kelvin. |
| kbyte | Kilobyte ($10^3$ byte). |
| m | Meter. |
| MHz | Megahertz ($10^6$ Hertz). |
| nm | Nanometer ($10^{-9}$ Meter). |
| s | Second. |
| Tbps | Terabits per second ($10^{12}$ bits per second). |
| V | Volt. |
| W | Watt. |

# Nomenclature

### Natural constants

| | |
|---|---|
| $e$ | Euler constant ($e = 2.718281828$). |
| $\widetilde{e}$ | Euler-Mascheroni constant ($\widetilde{e} = 0.5772156649$). |
| $\hbar$ | Reduced Planck constant ($\hbar = 1.054571628 \cdot 10^{34}$ Js). |
| $j$ | Imaginary unit ($j = \sqrt{-1}$). |
| $\mathrm{k_B}$ | Boltzmann constant ($\mathrm{k_B} = 1.38065 \cdot 10^{-23}$ J/K). |
| $\pi$ | Mathematical constant ($\pi = 3.141592653$). |

### Operators

| | |
|---|---|
| $* a$ | Convolution with $a$. |
| $\uparrow a$ | $a$-fold upsampling. |
| $\downarrow a$ | $a$-fold downsampling. |
| $\mathfrak{z}^{-a}$ | Discrete time delay by $a$ samples. |
| $a \to b$ | Parameter $a$ approaches the value $b$. |
| $A \to B$ | Mapping between two random variables $A$ and $B$. |
| $a \in \mathbb{B}$ | $a$ is an element of the set $\mathbb{B}$. |
| $a \overset{\text{i.i.d.}}{\sim} \mathrm{B}$ | $a$ is drawn i.i.d. according to the distribution B. |
| $(\cdot)\, \forall\, a \in \mathbb{B}$ | The expression $(\cdot)$ holds for all $a$ that are elements of the set $\mathbb{B}$. |
| $(\cdot)^{-1}$ | Inverse of a scalar, vector or matrix. |
| $(\cdot)^*$ | Complex conjugate of a complex-valued scalar, vector or matrix. |
| $\lvert \cdot \rvert$ | Magnitude of a complex-valued scalar or a real-valued scalar. |
| $\sphericalangle(\cdot)$ | Phase of a complex-valued scalar. |
| $\binom{a}{b}$ | Binomial coefficient ($a$ choose $b$). |
| $a\big\rvert_b$ | Value of $a$ at position $b$. |
| $\lim\limits_{b \to c} a$ | Limit of $a$ when $b$ approaches $c$. |
| $\max\limits_b a$ | Maximum of $a$ with respect to $b$. |
| $\min\limits_b a$ | Minimum of $a$ with respect to $b$. |
| $\min(a; b)$ | Minimum of $a$ and $b$. |

| | |
|---|---|
| $(\cdot) \bmod b$ | Modulo operator (remainder of the devision by $b$). |
| $\mathfrak{Re}\{\cdot\}$, $\mathfrak{Im}\{\cdot\}$ | Real and imaginary parts of a complex-valued scalar, vector or matrix. |
| $\partial(\cdot)/\partial a$ | Partial derivative with respect to $a$. |
| $\partial^2(\cdot)/\partial^2 a$ | Second order partial derivative with respect to $a$. |
| $\partial^2(\cdot)/\partial a \partial b$ | Second order partial derivative with respect to $a$ and $b$. |

**General functions**

| | |
|---|---|
| $\lceil\cdot\rceil$ | Ceiling function. |
| $\lfloor\cdot\rfloor$ | Floor function. |
| $\cos(\cdot)$ | Cosine function. |
| $\exp(\cdot)$ | Exponential function ($\exp(a) = e^a$). |
| $\mathrm{G}(a,\, b)$ | Incomplete Gamma function of $a$ with parameter $b$. |
| $\mathrm{I}_0(\cdot)$ | Modified Bessel function of zeroth order. |
| $\log_a(\cdot)$ | Logarithm to the base $a$. |
| $\mathrm{rect}(\cdot)$ | Rectangular function. |
| $\mathrm{sgn}(\cdot)$ | Sign function. |
| $\sin(\cdot)$ | Sine function. |
| $\mathrm{Z}(\cdot)$ | Step function. |
| $\delta(\cdot)$ | Dirac Delta function. |
| $\Phi(\cdot)$, $\Phi^{-1}(\cdot)$ | Standard Gaussian CDF, and its inverse. |
| $\mathcal{Q}(b,a)$, $\mathcal{Q}^{-1}(b,a)$ | First order Marcum Q-function of $a$ with parameter $b$, and its inverse. |
| $\Upsilon(\cdot)$, $\Upsilon^{-1}(\cdot)$ | Binary entropy function, and its inverse. |

**Matrix and vector operations**

| | |
|---|---|
| $[\,\cdot\,]_{n,\,n'}$ | Matrix element in the $n$-th row and the $n'$-th column. |
| $[\,\cdot\,]_{n,\,:}$ | Vector of the $n$-th row of a matrix. |
| $[\,\cdot\,]_n$ | Vector element in the $n$-th row. |
| $(\cdot)^{\mathrm{T}}$ | Transpose of a vector or matrix. |
| $(\cdot)^{\mathrm{H}}$ | Hermitian of a vector or matrix. |
| $\lvert\lvert \cdot \rvert\rvert^2$ | L2-Norm of a vector. |
| $\det(\cdot)$ | Determinant of a matrix. |
| $\mathrm{diag}(\boldsymbol{A})$ | Matrix $\boldsymbol{A}$ with all off-diagonal elements set to zero. |
| $\mathrm{nondiag}(\boldsymbol{A})$ | Matrix $\boldsymbol{A}$ with all diagonal elements set to zero. |
| $\mathrm{tr}(\cdot)$ | Trace of a matrix. |
| $\nabla_{\boldsymbol{b}}\, a$ | Gradient vector of $a$ with respect to the elements of the vector $\boldsymbol{b}$. |
| $\mathbf{R}_{\boldsymbol{a}\boldsymbol{a}^{\mathrm{H}}}$ | Covariance matrix of a vector $\boldsymbol{a}$ ($\mathbf{R}_{\boldsymbol{a}\boldsymbol{a}^{\mathrm{H}}} = \mathrm{E}_{\boldsymbol{a}}\{\boldsymbol{a}\cdot\boldsymbol{a}^{\mathrm{H}}\}$). |
| $\mathbf{R}_{\boldsymbol{a}\boldsymbol{b}^{\mathrm{H}}}$ | Cross-covariance matrix of two vectors $\boldsymbol{a}$ and $\boldsymbol{b}$ ($\mathbf{R}_{\boldsymbol{a}\boldsymbol{b}^{\mathrm{H}}} = \mathrm{E}_{\boldsymbol{a},\boldsymbol{b}}\{\boldsymbol{a}\cdot\boldsymbol{b}^{\mathrm{H}}\}$). |

**Sets**

| | |
|---|---|
| $\{a,\, a{+}1, \ldots, b\}$ | Index set ranging from index $a$ to index $b$. |
| $\mathbb{C}$ | Set of complex-valued numbers. |
| $\mathbb{N}$ | Set of natural numbers. |
| $\mathbb{R}$ | Set of real-valued numbers. |
| $\mathbb{Z}$ | Set of integer numbers. |

**Indexes and integer delays**

| | |
|---|---|
| $i, i'$ | Index for TI data converter branches, fractional parts of a symbol interval or fractionally-spaced paths of a channel. |
| $i_\mathrm{c}$ | Index for multiple identical channels. |
| $\mathtt{i}$ | Index for previous iterations of the Cutting-Plane algorithm. |
| $k,\, k'$ | Symbol time index. |
| $k_\mathrm{delay}$ | Delay between transmitted and received symbols. |
| $k_{\mathrm{delay,\,max}},\, k_{\mathrm{delay,\,opt}}$ | Maximum and optimal delay between transmitted and received symbols. |
| $k_{\mathrm{max},\,i}$ | Index of the strongest coefficient of the overall channel impulse response or pre-equalizer in the $i$-th fractionally-spaced path. |
| $l,\, l'$ | Index for possible transmit symbols (channel inputs). |
| $l_k$ | Index for possible transmit symbols at time index $k$. |
| $n,\, n',\, n''$ | Sample time index. |
| $n_\mathrm{delay}$ | Sample delay of the start of the detection interval within a symbol pulse. |
| $n_{k,\,1}, \ldots, n_{k,\,\iota}$ | Sample time indexes in a received sample sequence belonging to a symbol that has been transmitted at symbol time index $k$ ($1 \leq \iota \leq N$). |
| $\mathtt{n}$ | Index for the current iteration of the Cutting-Plane algorithm. |
| $m,\, m'$ | Quantization level index. |
| $m_\mathrm{I},\, m'_\mathrm{I}, m_\mathrm{Q},\, m'_\mathrm{Q}$ | Index for possible in-phase and quadrature-phase received signal amplitudes (in-phase and quadrature-phase channel outputs). |
| $\alpha$ | Index for possible received symbol vectors (channel output vectors). |
| $\kappa,\, \kappa'$ | Index for possible transmit symbol vectors (channel input vectors). |
| $\lambda$ | Index for possible received signal amplitudes (channel outputs). |
| $\lambda_n$ | Index for possible received signal amplitudes at sample time index $n$. |

**Numbers and lengths**

| | |
|---|---|
| $K$ | Number of symbols in a sequence. |
| $\mathcal{K}$ | Number of stages or branches of a data converter. |
| $L$ | Number of possible channel inputs, or cardinality of modulation schemes. |
| $L_\mathrm{opt}$ | Optimal number of possible channel inputs. |
| $\Lambda$ | Number of possible channel outputs or received signal amplitudes. |
| $M,\, M'$ | Number of quantization levels, or number of digits. |

| | |
|---|---|
| $M_{\mathrm{opt}}$ | Optimized number of quantization levels. |
| $N$ | Number of samples. |
| $N_{\mathrm{c}}$ | Number of parallel channels. |
| $N_{\mathrm{ch}}$ | Length of the discrete time impulse response of the overall channel. |
| $N_{\mathrm{ch},\,i}$ | Length of the discrete time impulse response of the overall channel in the $i$-th fractionally-spaced path. |
| $N_{\mathrm{GI}}$ | Minimum guard interval length. |
| $N_{\mathrm{eq}}$, $N'_{\mathrm{eq}}$ | (Pre-)equalizer length. |
| $N_{\mathrm{eq},\,i}$ | (Pre-)equalizer length in the $i$-th fractionally-spaced path. |
| $N_{\mathrm{Rx}}$ | Length of the discrete time impulse response of the receiver. |
| $\Sigma_b$ | Number of simulations carried out for $b$. |
| $\Sigma_{a\|b}$ | Number of occurrences of $a$ given $b$ in a simulation. |

**Frequency and time parameters**

| | |
|---|---|
| $f$ | Frequency variable. |
| $f_{3\,\mathrm{dB}}$ | 3 dB cut-off frequency of a filter. |
| $f_{\mathrm{Rx}}$ | Receiver bandwidth limit. |
| $f_{\mathrm{s}}$, $f'_{\mathrm{s}}$ | Sampling rate. |
| $f_{\mathrm{s,\,ADC}}$, $f_{\mathrm{s,\,DAC}}$ | Sampling rate of ADCs and DACs. |
| $f_{\mathrm{s,\,max}}$, $f_{\mathrm{s,\,opt}}$ | Maximum and optimized sampling rate. |
| $f_{\mathrm{symb}}$ | Symbol rate. |
| $\mathcal{F}$ | Quantum-theoretic frequency constant. |
| $t$, $t'$, $t''$ | Time variable. |
| $\Delta t$ | Time uncertainty. |
| $T_{\mathrm{s}}$ | Sampling time interval. |
| $T_{\mathrm{s,\,ADC}}$, $T_{\mathrm{s,\,DAC}}$ | Sampling time interval of ADCs and DACs. |
| $\Delta T_i$ | Sampling time delay in the $i$-th branch of a TI data converter. |
| $\tau$ | Time shift. |
| $\tau_{\mathrm{s}}$ | Sampling time offset. |
| $\xi$ | Oversampling ratio. |
| $\xi_w$ | Oversampling ratio for the discrete time representation of white noise. |

**Quantization characteristics and related parameters**

| | |
|---|---|
| $\boldsymbol{a}$ | Vector of quantization thresholds. |
| $a_m$ | Quantization threshold with index $m$. |
| $\widetilde{a}_m$ | Relative quantization threshold with index $m$. |
| $\widetilde{a}_{\mathrm{I},\,m}$, $\widetilde{a}_{\mathrm{Q},\,m}$, $\widetilde{a}_{\mathrm{I/Q},\,m}$ | Relative in- and quadrature-phase quantization thresholds with index $m$. |
| $\widetilde{a}_{\mathrm{c}}$ | Relative center of the quantization input range. |

| | |
|---|---|
| $\Delta a$ | Quantization interval size. |
| $\Delta\widetilde{a}$, $\Delta\widetilde{a}_{\mathrm{opt}}$ | Relative quantization interval size, and its optimum. |
| $\Delta\widetilde{a}_{\mathrm{ML}}$ | Relative quantization interval size of the maximum likelihood metric. |
| $B$ | Quantization resolution. |
| $B_{\mathrm{coarse}}$, $B_{\mathrm{fine}}$ | Coarse and fine quantization resolution in a segmented data converter. |
| ENOB, $\mathrm{ENOB}_{\mathrm{opt}}$ | Effective number of bits, and its optimum. |
| $\boldsymbol{q}$ | Vector of quantization levels. |
| $q_m$ | Quantization level with index $m$. |
| $\widetilde{q}_m$ | Relative quantization level with index $m$. |
| $\Delta q$ | Quantization level spacing. |
| $\Delta\widetilde{q}$, $\Delta\widetilde{q}_{\mathrm{opt}}$ | Relative quantization level spacing, and its optimum. |
| $\mathrm{Q}_{\boldsymbol{a}}^{\boldsymbol{q}}(\cdot)$ | Quantization function with the thresholds and levels given by $\boldsymbol{a}$ and $\boldsymbol{q}$. |
| $\mathrm{Q}_{\boldsymbol{a},\,\mathrm{ADC}}^{\boldsymbol{q}}(\cdot)$, $\mathrm{Q}_{\boldsymbol{a},\,\mathrm{DAC}}^{\boldsymbol{q}}(\cdot)$ | Quantization function of ADCs and DACs. |
| $\beta_{\mathrm{in}}$, $\beta_{\mathrm{out}}$ | Input and output scaling factors of a quantization characteristic. |
| $\beta_{\mathrm{in},\,i}$, $\beta_{\mathrm{out},\,i}$ | Input and output scaling factors in the $i$-th fractionally-spaced path. |
| $\mathfrak{B}_{\mathrm{in}}$, $\mathfrak{B}_{\mathrm{out}}$ | Diagonal matrices of the input and output scaling factors $\beta_{\mathrm{in},\,i}$ and $\beta_{\mathrm{out},\,i}$. |
| $\hat{\boldsymbol{\chi}}_\alpha$, $\check{\boldsymbol{\chi}}_\alpha$ | Vectors of lower and upper 1-bit quantization thresholds for the output vector symbol $\underline{\mathbf{y}}_\alpha$. |

**Physical quantities of signals and data converters**

| | |
|---|---|
| $\mathcal{E}$ | Total energy span for the representation of signal amplitudes. |
| $\overline{\mathcal{E}}$ | Energy of a quantum system. |
| $\Delta\mathcal{E}$ | Energy uncertainty. |
| $\mathrm{FOM}_1$, $\mathrm{FOM}_2$ | Figures of merit for ADCs. |
| $\mathcal{I}$ | Current. |
| $\mathcal{V}_{\mathrm{eff}}$ | Effective voltage (CMOS technology parameter). |
| $\Delta\mathcal{V}$ | Voltage step size. |
| $\mathcal{C}$ | Capacitance. |
| $\mathcal{C}_{\mathrm{min}}$ | Minimum capacitance (CMOS technology parameter). |
| $\mathcal{P}_{\mathrm{ADC}}$, $\mathcal{P}_{\mathrm{DAC}}$ | Power dissipation of ADCs and DACs. |
| $\mathcal{P}_{\mathrm{ADC,\,lim}}$ | ADC power dissipation limit. |
| $\mathcal{P}_{\mathrm{ADC,\,min}}$ | Minimized ADC power dissipation. |
| $\mathcal{P}_{\mathrm{ADC,\,ref}}$ | Reference ADC power dissipation. |
| $\mathcal{P}_{\mathrm{flash\,ADC}}$ | Power dissipation limit of flash ADCs. |
| $\mathcal{P}_{\mathrm{pipeline\,ADC}}$ | Power dissipation limit of pipeline ADCs. |
| $\mathcal{T}_{ADC}$, $\mathcal{T}_{DAC}$ | Energy consumption per converted bit of ADCs and DACs. |
| $\nu$ | ADC power dissipation parameter (sampling frequency exponent). |
| $\sigma_{\mathrm{th}}$ | Standard deviation of the thermal noise voltage of integrated capacitors. |
| $\vartheta$ | Temperature. |

### Signals and symbol sequences

| | |
|---|---|
| $v(t)$ | Analog transmit signal. |
| $w(t)$ | Analog white noise signal. |
| $\widetilde{w}(t)$ | Analog band-limited noise signal. |
| $x(t)$ | Analog received signal. |
| $y(t)$ | Continuous time quantized received signal. |
| $r[k]$ | Detected symbol sequence. |
| $s[k]$ | Transmit symbol sequence. |
| $u[n]$ | Un-quantized transmit signal samples (DAC input signal). |
| $u_i[k]$ | Un-quantized transmit signal samples of the $i$-th fractionally-spaced path. |
| $v[n]$ | Quant. transmit signal samples (scaled discrete time DAC output signal). |
| $v_i[k]$ | Quantized transmit signal samples of the $i$-th fractionally-spaced path. |
| $x[n]$ | Un-quantized received signal samples. |
| $x_i[k]$ | Un-quantized received signal samples of the $i$-th fractionally-spaced path. |
| $w[n]$ | Noise signal samples. |
| $\overline{w}_i[k]$ | Filtered noise signal samples of the $i$-th fractionally-spaced path. |
| $w_{\mathrm{Q}}[n]$ | Quantization distortion signal samples. |
| $w_{\mathrm{Q,i}}[k]$ | Quantization distortion signal samples of the $i$-th fractionally-spaced path. |
| $y[n]$ | Quantized received signal samples (ADC output signal). |
| $y_i[k]$ | Quantized received signal samples of the $i$-th fractionally-spaced path. |
| $z[k]$ | Received symbol sequence. |
| $z_i[k]$ | Received symbol sequence part in the $i$-th fractionally-spaced path. |

### Amplitudes of signals and symbols

| | |
|---|---|
| $s$, $s'$ | Transmit symbol amplitude (channel input). |
| $s_{\mathrm{I}}$, $s_{\mathrm{Q}}$, $s_{\mathrm{I/Q}}$ | In-phase and quadrature-phase of the transmit symbol amplitude. |
| $s_{n_{\mathrm{c}}}$ | Channel input of the $n_{\mathrm{c}}$-th parallel channel. |
| $x$ | Un-quantized received signal amplitude (quantizer input amplitude). |
| $x_i$ | Un-quantized received signal amplitude of the $i$-th fract.-spaced path. |
| $x_{\mathrm{I}}$, $x_{\mathrm{Q}}$, $x_{\mathrm{I/Q}}$, $x'_{\mathrm{I/Q}}$ | In- and quadrature-phase of the un-quantized received signal amplitude. |
| $u$ | Un-quantized transmit signal amplitude (quantizer input amplitude). |
| $u_i$ | Un-quantized transmit signal amplitude of the $i$-th fract.-spaced path. |
| $v$ | Quantized transmit signal amplitude (scaled quantizer output amplitude). |
| $y$ | Quantized received signal amplitude (scaled quantizer output amplitude). |
| $y_{\mathrm{I}}$, $y_{\mathrm{Q}}$ | In-phase and quadrature-phase of the quantized received signal amplitude. |
| $y_{\Sigma}$ | Sum of the quantized received signal amplitudes per transmit symbol. |
| $y_{\Sigma,\mathrm{I}}$, $y_{\Sigma,\mathrm{Q}}$ | In-phase and quadrature-phase of the sum of the quantized received signal amplitudes per transmit symbol. |

| | |
|---|---|
| $z$ | Received symbol amplitude. |
| $w$ | Noise signal amplitude. |
| $\breve{w}_i$ | Effective distortion signal amplitude in the $i$-th fractionally-spaced path. |
| $w_{\mathrm{Q}}$ | Quantization distortion signal amplitude. |
| $w_{\mathrm{Q},\,\xi}$ | Quantization distortion signal amplitude with $\xi$-fold oversampling. |
| $w_{\mathrm{Q},\,i}$ | Quantization distortion signal amplitude of the $i$-th fract.-spaced path. |
| $\varpi$ | Channel input amplitude affected by the channel phase. |
| $\varpi_{\mathrm{I}}$, $\varpi_{\mathrm{Q}}$ | In-phase and quadrature-phase of the channel input amplitude affected by the channel phase. |
| $\psi_s$ | Phase of the transmit symbol amplitude $s$ ($\psi_s = \sphericalangle(s)$). |
| $\upsilon_s$ | Magnitude of the transmit symbol amplitude $s$ ($\upsilon_s = \lvert s \rvert^2$). |
| $\upsilon_{s\mid\psi_s}$ | Magnitude of the transmit symbol amplitude $s$ for a given phase $\psi_s$. |
| $\mathsf{s}$, $\mathsf{s}'$ | Possible transmit symbol. |
| $\mathsf{s}_l$ | Possible transmit symbol with index $l$. |
| $\mathsf{s}_{\mathrm{I},\,l}$, $\mathsf{s}_{\mathrm{Q},\,l}$ | In-phase and quadrature-phase of the possible transmit symbol with index $l$. |
| $\mathsf{v}_l$ | Possible quantized transmit signal amplitude with index $l$. |
| $\mathsf{y}_\lambda$ | Possible quantized received signal amplitude with index $\lambda$. |
| $\mathsf{y}_{\mathrm{I},\,\lambda}$, $\mathsf{y}_{\mathrm{Q},\,\lambda}$ | In-phase and quadrature-phase of the possible quantized received signal amplitude with index $\lambda$. |
| $\mathsf{y}_\Sigma$ | Possible sum of the quant. received signal amplitudes per transmit symbol. |
| $\mathsf{y}_{\Sigma,\,\mathrm{I}}$, $\mathsf{y}_{\Sigma,\,\mathrm{I}}$ | In-phase and quadrature-phase of the possible sum of the quantized received signal amplitudes per transmit symbol. |
| $\mathsf{z}_\lambda$ | Possible received symbol amplitude with index $\lambda$. |

**Vectors of signals and symbols**

| | |
|---|---|
| $\boldsymbol{s}$ | Transmit symbol vector. |
| $\underline{\boldsymbol{s}}$ | Transmit symbol sub-vector. |
| $\boldsymbol{u}$ | Vector of un-quantized transmit signal samples. |
| $\boldsymbol{v}$ | Vector of quantized transmit signal samples. |
| $\boldsymbol{v}_{\mathrm{I}}$, $\boldsymbol{v}_{\mathrm{Q}}$ | In- and quadrature-phase vectors of quantized transmit signal samples. |
| $\boldsymbol{w}$ | Vector of noise signal samples. |
| $\underline{\boldsymbol{w}}$ | Sub-vector of noise signal samples. |
| $\boldsymbol{w}_{\mathrm{Q}}$ | Vector of quantization distortion signal samples. |
| $\boldsymbol{x}$ | Vector of un-quantized received signal samples. |
| $\underline{\boldsymbol{x}}$ | Sub-vector of un-quantized received signal samples. |
| $\boldsymbol{y}$ | Vector of quantized received signal samples. |
| $\boldsymbol{y}_{\mathrm{I}}$, $\boldsymbol{y}_{\mathrm{Q}}$ | In- and quadrature-phase vectors of quantized received signal samples. |
| $\underline{\boldsymbol{y}}$ | Sub-vector of quantized received signal samples. |

| | |
|---|---|
| $\underline{\boldsymbol{y}}_k$ | Sub-vector of quantized received signal samples belonging to the symbol that has been transmitted at symbol time index $k$. |
| $\boldsymbol{z}$ | Received symbol vector. |
| $\mathbf{s}$ | Possible transmit symbol vector. |
| $\mathbf{s}_\kappa$ | Possible transmit symbol vector with index $\kappa$. |
| $\mathbf{y}_\alpha$ | Possible vector of quantized received signal amplitudes with index $\alpha$. |
| $\mathbf{y}_{\mathrm{I},\alpha}$, $\mathbf{y}_{\mathrm{Q},\alpha}$ | Possible in-phase and quadrature-phase vectors of quantized received signal amplitudes with index $\alpha$. |
| $\underline{\mathbf{y}}_\alpha$ | Possible sub-vector of quantized received signal amplitudes with index $\alpha$. |

**Random variables and random vectors**

| | |
|---|---|
| $S$, $S'$ | Random variable of transmit symbols. |
| $\boldsymbol{S}$ | Random vector of transmit symbols. |
| $U$ | Random variable of un-quantized transmit signal amplitudes. |
| $V$ | Random variable of quantized transmit signal amplitudes. |
| $Y$ | Random variable of quantized received signal amplitudes. |
| $\boldsymbol{Y}$ | Random vector of quantized received signal amplitudes. |
| $\underline{\boldsymbol{Y}}$ | Random sub-vector of quantized received signal amplitudes. |
| $Y_\Sigma$ | Random variable of sum the of quantized received signal amplitudes per transmit symbol. |
| $Z$ | Random variable of received symbols. |
| $\Pi$ | Random variable of channel inputs affected by the channel phase. |

**Channel characteristics**

| | |
|---|---|
| $g(t)$, $G(f)$ | Continuous time impulse responses, and respective frequency response. |
| $g_{\mathrm{ch}}(t)$, $g_{\mathrm{ch}}[n]$ | Continuous and discrete time impulse response of the overall channel. |
| $\boldsymbol{g}_{\mathrm{ch}}$, $\boldsymbol{G}_{\mathrm{ch}}$, $\underline{\boldsymbol{G}}_{\mathrm{ch}}$ | Vector and convolution matrices of the discrete time impulse response of the overall channel. |
| $\breve{g}_{\mathrm{ch}}(t)$ | Continuous time impulse response of the overall channel without the signal integration of the ADCs at the receiver. |
| $g_{\mathrm{Rx}}(t)$, $g_{\mathrm{Rx}}[n]$ | Continuous and discrete time impulse responses of the receiver. |
| $\boldsymbol{g}_{\mathrm{Rx}}$, $\boldsymbol{G}_{\mathrm{Rx}}$ | Vector and convolution matrix of the discrete time impulse response of the receiver. |
| $g_{\mathrm{Tx}}(t)$ | Continuous time impulse response of the transmitter. |
| $g_{\mathrm{RF}}(t)$ | Continuous time impulse response of the radio channel. |
| $\boldsymbol{G}_\sqcap$, $\breve{\boldsymbol{G}}_\sqcap$ | Convolution matrices of the rectangular DAC output pulse shape. |
| $\mathcal{N}_0$ | Noise PSD level. |
| $\phi$ | Frequency-flat channel phase. |
| $\phi_i$ | Effective phase offset in the $i$-th fractionally-spaced path. |

| | |
|---|---|
| $\bar{\phi}$, $\breve{\phi}$ | Static LOS and random non-LOS phase of a fading channel. |
| $\Gamma$ | Rice factor of a fading channel. |
| $\theta$ | Frequency-flat channel gain. |
| $\theta_i$ | Effective channel gain in the $i$-th fractionally-spaced path. |
| $\theta_{\mathrm{out}}$, $\theta_{\mathrm{out},\,\phi}$ | Outage channel gain: in general and for a given channel phase $\phi$. |
| $\bar{\theta}$, $\breve{\theta}$ | Static LOS and random non-LOS channel gain of a fading channel. |
| $\widetilde{\theta}$ | Channel gain normalized to the standard deviation $\sigma_\theta$. |
| $\widetilde{\theta}_{\mathrm{out}}$ | Outage channel gain normalized to standard deviation $\sigma_\theta$. |
| $\Omega$ | Maximum average transmit power. |
| $\Omega_{\mathrm{real}}$, $\Omega_{\mathrm{peak}}$ | Maximum average and peak transmit power of a real-valued channel. |

**Probabilities, probability distributions and PDFs**

| | |
|---|---|
| $\mathrm{B}(a,\,b)$ | Binomial distribution with parameters $a$ and $b$. |
| $\mathrm{N}(\mu_a, \sigma_a^2)$ | Gaussian distribution with mean $\mu_a$ and variance $\sigma_a^2$. |
| $\mathrm{N}_{\mathbb{C}}(\mu_a, \sigma_a^2)$ | Complex Gaussian distribution with mean $a$ and variance $b$. |
| $\mathrm{p}_b(a)$, $\mathrm{p}'_b(a)$ | PDF of $b$ at position $a$. |
| $\mathrm{p}_{c,\,\ldots,\,d}(a, \ldots, b)$ | Joint PDF of $c$ to $d$ at positions $a$ to $b$. |
| $\mathrm{p}_{c\mid d}(a\mid b)$ | Conditional PDF of $c$ given $d$ at positions $a$ and $b$. |
| $\mathrm{p}_{\mathrm{real}}(a)$ | Real-valued channel input PDF at position $a$. |
| $\mathrm{P}_{a,\,b}$ | Probability of a 9-QAM symbol $c$ with in-phase index $a = \mathrm{sgn}(\mathfrak{Re}\{c\})$ and quadrature-phase index $b = \mathrm{sgn}(\mathfrak{Im}\{c\})$. |
| $\mathrm{P}_{\mathrm{out}}$, $\mathrm{P}_{\mathrm{out,\,opt}}$ | Outage probability, and its optimum to maximize the capacity with outage. |
| $\mathrm{P}_{\mathrm{out},\,\phi}$ | Outage probability for a given channel phase $\phi$. |
| $\mathrm{Pr}(a)$ | Probability (distribution) of a random event $a$. |
| $\mathrm{Pr}(a\mid b)$ | Conditional probability (distribution) of a random event $a$ given $b$. |
| $\mathrm{Pr}_{\mathtt{i}}(\cdot)$ | Channel input probability distribution computed in the $\mathtt{i}$-th iteration of the Cutting-Plane algorithm. |
| $\overline{\mathrm{Pr}}_K(\cdot\mid\cdot)$ | Marginal transition probabilities of a DMC with input vectors of length $K$. |
| $\varsigma_{\mathrm{I}}$, $\varsigma_{\mathrm{Q}}$ | In- and quadrature-phase transition probability factors (see (5.9), pg. 73). |
| $\zeta_{\mathrm{I}}$, $\zeta_{\mathrm{Q}}$ | In- and quadrature-phase transition probability factors (see (6.6), pg. 123). |

**Statistical measures**

| | |
|---|---|
| $\mathrm{E}_b\{a\}$ | Expectation of $a$ with respect to the PDF of $b$. |
| $\mathrm{E}_{b\mid c}\{a\}$ | Expectation of $a$ with respect to the conditional PDF of $b$ given $c$. |
| $\eta_a$ | Peak-to-average-power ratio ($\eta_a = \max\, \lvert a\rvert^2 / \sigma_a^2$). |
| $\mu_a$ | Mean value ($\mu_a = \mathrm{E}_a\{a\}$). |
| $\sigma_a$ | Standard deviation ($\sigma_a = \sqrt{\mathrm{E}_a\{\lvert a - \mu_a\rvert^2\}}$). |
| $\sigma_{a,\,n}$ | Standard deviation of $a$ at the sample time index $n$. |
| $\sigma_{a,\,i}$ | Standard deviation of $a$ in the $i$-th fractionally-spaced path of a channel. |

### Signal distortion measures

| | |
|---|---|
| $\mathrm{d}(a;b)$ | Distortion metric between $a$ and $b$. |
| $\mathrm{D}(A;B)$ | Average distortion between two random variables $A$ and $B$. |
| $D$ | Maximum distortion. |
| $\mathrm{F}_R(\cdot)$ | Rate distortion function. |
| $\varepsilon$, $\varepsilon_{\min}$ | MSE and MMSE. |
| $\varepsilon_{\mathrm{Q}}$ | MSE of the quantization. |
| $\varepsilon_{\mathrm{Q,\,I}}$, $\varepsilon_{\mathrm{Q,\,Q}}$, $\varepsilon_{\mathrm{Q,\,I/Q}}$ | MSE of the in-phase and quadrature-phase quantization. |
| $\varepsilon_{\mathrm{Q},\,m}$ | Fractional MSE of the quantization in the $m$-th quantization interval. |
| $\varepsilon_{\mathrm{Q},\,n}$ | MSE of the quantization at sample time index $n$. |
| $\varepsilon_{\mathrm{Q},\,i}$, $\varepsilon_{\mathrm{Q,\,min},\,i}$ | MSE and MMSE of the quantization in the $i$-th fractionally spaced path. |
| $\gamma$ | SNR. |
| $\overline{\gamma}$ | Average SNR of a fading channel. |
| $\hat{\gamma}$ | Capacity maximizing SNR. |
| $\gamma_{\mathrm{eff}}$ | Effective SNR. |
| $\gamma_{\mathrm{eff,\,ZF}}$ | Effective SNR with ZF precoding. |
| $\gamma_{\mathrm{eff,\,RxWF}}$, $\gamma_{\mathrm{eff,\,TxWF}}$ | Effective SNR with receive or transmit WF channel (pre-)equalization. |
| $\gamma_{\mathrm{shift}}(a,\,b)$ | SNR shift as a function of $a$ and $b$. |
| $\gamma_{\mathrm{Q}}$ | SQNR. |
| $\gamma_{\mathrm{Q},\,\xi}$ | SQNR with $\xi$-fold oversampling. |
| $\gamma_{\mathrm{Q},\,n}$, $\breve{\gamma}_{\mathrm{Q},\,n}$ | SQNR at sample time index $n$, and at permuted sample time index $n$. |
| $\gamma_{\mathrm{Q},\,i}$ | SQNR in the $i$-th fractionally-spaced path. |
| $\boldsymbol{\mathfrak{T}}_{\mathrm{Q}}$, $\breve{\boldsymbol{\mathfrak{T}}}_{\mathrm{Q}}$ | Diagonal matrix of inverse SQNR values, and its permuted version. |

### Information-theoretic measures

| | |
|---|---|
| $\mathcal{E}_{\mathrm{bit}}$ | Received signal energy per transmitted information bit. |
| $\mathrm{C}$, $\mathrm{C}'$ | Channel capacity. |
| $\mathrm{C_I}$, $\mathrm{C_Q}$, $\mathrm{C_{I/Q}}$ | Channel capacity of the in-phase and quadrature-phase parts of a channel. |
| $\mathrm{C_{lb}}$, $\mathrm{C_{ub}}$ | Channel capacity lower and upper bounds. |
| $\mathrm{C}_{\mathrm{lb},\,\mathtt{n}}$, $\mathrm{C}_{\mathrm{ub},\,\mathtt{n}}$ | Channel capacity bounds after $\mathtt{n}$ iterations of the Cutting-Plane algorithm. |
| $\mathrm{C_{max}}$ | Channel capacity maximum. |
| $\mathrm{C}_{\mathrm{max},\,L}$ | Channel capacity maximum with $L$ equally-spaced DAC output levels. |
| $\mathrm{C}_N$ | Channel capacity for a blockwise transmission with block length $N$. |
| $\widetilde{\mathrm{C}}_N$ | Channel capacity for a blockwise tr. with block length $N$ and GI detection. |
| $\mathrm{C_{out}}$ | Channel capacity with outage. |
| $\mathrm{C_{PQN}}$ | Channel capacity approximation based on the PQN model. |
| $\mathrm{C_{real}}$ | Channel capacity of a real-valued channel. |
| $\mathrm{C_{ZF}}$ | Channel capacity with ZF precoding. |

| | |
|---|---|
| $\overline{\mathrm{C}}$, $\Delta\overline{\mathrm{C}}$ | Ergodic capacity of fading channels, and respective fading channel loss. |
| $\mathrm{F_C}(a;b)$ | Maximum channel capacity as a function of $a$ and $b$. |
| $\mathrm{H}(A)$ | Entropy of $A$. |
| $\mathrm{H}(A\|B)$ | Conditional entropy of $A$ given $B$. |
| $\mathrm{I}(\mathsf{a};B)$ | Kullback-Leibler divergence between $\mathsf{a}$ and $B$. |
| $\mathrm{I}(A;B)$ | Mutual information between $A$ and $B$. |
| $\mathrm{I}(A;B \mid C)$ | Mutual information between $A$ and $B$ given $C$. |
| $\Delta\mathrm{I}(A;B)$ | Improvement of the mutual information or spectral efficiency. |
| $\mathrm{I}_N(A;B)$ | Average mutual information between $A$ and $B$ per symbol, considering a blockwise symbol transmission with block length $N$. |
| $\widehat{\mathrm{I}}_{\mathtt{n}}(A;B)$ | Piecewise approximation of the mutual information in the $\mathtt{n}$-th iteration of the Cutting-Plane algorithm. |
| $\mathrm{I}_{\mathtt{i}}(\mathsf{a};B)$ | Kullback-Leibler divergence for the channel input distribution obtained in the $\mathtt{i}$-th iteration of Cutting-Plane algorithm. |
| $\mathrm{J}_m$ | Weighted information content of a signal amplitude level with index $m$. |
| $\mathrm{R_{out}}$, $\mathrm{R_{out,\,opt}}$ | Outage rate, and its optimum to maximize the capacity with outage. |
| $\mathcal{R}$ | Data rate. |
| $\mathcal{R}_{\mathrm{ADC}}$, $\mathcal{R}_{\mathrm{DAC}}$ | ADC output data rate, and DAC input data rate. |
| $\mathcal{R}_{\max}$ | Maximum information rate. |
| $\mathcal{R}_{\mathrm{opt}}$ | Maximum information rate with an optimized amplitude resolution. |
| $\Psi$, $\Psi_{\max}$ | Spectral efficiency, and its maximum. |

**(Pre-)equalization and precoding characteristics**

| | |
|---|---|
| $\mathfrak{b}_{\mathrm{RxWF}}$, $\mathfrak{b}_{\mathrm{TxWF}}$ | Bias after receive and transmit WF (pre-)equalization. |
| $\mathfrak{g}[n]$ | (Pre-)equalizer coefficients. |
| $\mathfrak{g}_{\mathrm{MF}}[n']$ | Matched receive filter coefficients. |
| $\boldsymbol{\mathfrak{g}}$ | Vector of (pre-)equalizer coefficients. |
| $\mathfrak{g}_i[k]$ | (Pre-)equalizer coefficients of the $i$-th fractionally-spaced path. |
| $\mathfrak{g}_{\mathrm{RxWF},\,i}[k]$ | Receive WF equalizer coefficients of the $i$-th fractionally-spaced path. |
| $\mathfrak{g}_{\mathrm{TxWF},\,i}[k]$ | Transmit WF pre-equalizer coeff. of the $i$-th fractionally-spaced path. |
| $\boldsymbol{\mathfrak{g}}_{\mathrm{RxWF}}$, $\boldsymbol{\mathfrak{g}}_{\mathrm{TxWF}}$ | Vectors of receive and transmit WF (pre-)equalizer coefficients. |
| $\boldsymbol{\mathfrak{G}}$ | Precoding matrix, or convolution matrix of pre-equalizer coefficients. |
| $\boldsymbol{\mathfrak{G}}_{\mathrm{ZF}}$, $\boldsymbol{\mathfrak{G}}_{\mathrm{WF}}$ | ZF and WF precoding matrices. |
| $\boldsymbol{\mathfrak{h}}$ | Unscaled vector of transmit WF pre-equalizer coefficients. |
| $\beta_{\mathrm{Rx}}$ | Received signal scaling factor. |
| $\beta_{\mathrm{Rx,\,WF}}$ | Received signal scaling factor for WF precoding. |
| $\beta_{\mathrm{Rx,\,TxWF}}$ | Received signal scaling factor for transmit WF pre-equalization. |
| $\widetilde{\beta}_{\mathrm{Rx}}$ | Received signal scaling factor that combines $\beta_{\mathrm{Rx,\,WF}}$ or $\beta_{\mathrm{Rx,\,TxWF}}$ with an optimized quantization input scaling factor. |

**Miscellaneous**

| | |
|---|---|
| $\infty$ | Infinity. |
| $\mathbf{0}$, $\underline{\mathbf{0}}$ | Matrices of all zeros. |
| $b_{L\text{-QAM}}$ | Scaling factor of $L$-QAM symbol constellations with unit symbol variance. |
| $\boldsymbol{d}$ | Delay vector. |
| $\boldsymbol{\mathfrak{D}}$ | Downsampling matrix. |
| $\boldsymbol{I}$ | Identity matrix. |
| $\ell$, $\mathrm{L}(\cdot)$ | Lagrange variable, and Lagrange function. |
| $\varsigma$, $\mathrm{F}_{\varsigma}(\cdot)$ | Channel input constraint, and respective function. |
| $\mathcal{L}$ | Likelihood parameter. |
| $\boldsymbol{\mathfrak{U}}$, $\widetilde{\boldsymbol{\mathfrak{U}}}$ | Upsampling matrices. |
| $\mathfrak{S}_n$ | Cyclic shift matrix that rotates the elements of a vector by $n$ positions. |
| $\boldsymbol{A}$, $\boldsymbol{b}$, $\boldsymbol{c}$, $\boldsymbol{f}$<br>$\boldsymbol{p}$, $\boldsymbol{p}_{\mathrm{lb}}$, $\boldsymbol{p}_{\mathrm{ub}}$ | Parameter matrix and vectors of the linear program of the Cutting-Plane algorithm (see (B.21), pg. 195). |

# Chapter 1

# Introduction

## 1.1 Wireless Data Transmission

Over the last decades, wireless data transmission has become an integral part of human society. Wireless communications systems have found their way into almost every area of life. They add to an increased quality of life and play in important role in public infrastructure. The great success of these systems motivates ever new applications. Wireless data transmission does not only provide the flexibility to communicate with mobile devices, it can even mitigate the limitations and costs of conventional wire-based systems.

An example for the latter is the replacement of copper strips in computer racks using steerable radio beams. This can reduce the wiring complexity while still providing more flexible data links between the circuits mounted on different computer boards. Other emerging applications are, e.g., an ultra-fast wireless file transfer between any type of business or multimedia equipment, and wide-area wireless sensor networks that connect billions of battery-driven sensor devices to the Internet from every place all over the world. This is depicted in Figure 1.1.

Referring to these emerging applications, wireless data transmission faces two major challenges: The first challenge is the demand for ever higher data rates to be supported. A solution to this is the utilization of ever larger frequency bands. Only recently, regulatory bodies around the world have made available up to 9 GHz of bandwidth in the 60 GHz frequency band. Using this large amount of bandwidth, upcoming wireless standards will allow for data rates of several Gbps [ECM08, IEE09, IEE11]. This advancement is even expected to open the gate for data rate requirements beyond 1 Tbps [FGK11]. The second challenge, which gains more and more importance, is the constraint for a minimum energy consumption of the devices. This is driven by the impact of an ever growing device number on the world's ecosystem, but it also relates to

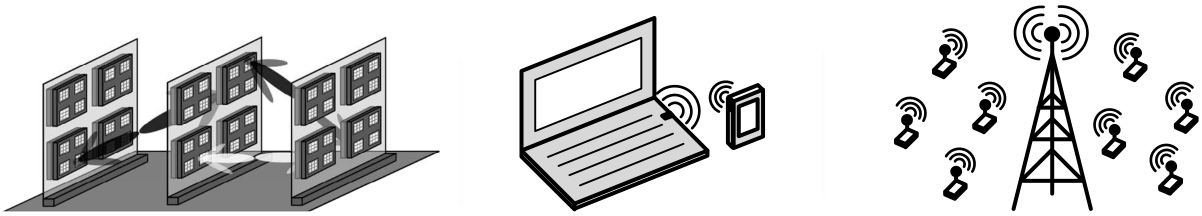

(a) Wireless links in computer racks. (b) Ultra-fast wireless file transfer. (c) Wireless sensor networks.

Figure 1.1: Emerging applications of wireless data transmission.

maximizing the operating time of battery-driven devices. Wireless system designs that address these challenges require a joint optimization of the system and transceiver architecture, with a strong focus on the transceiver hardware that is limiting the data rate and dominating the energy consumption. Considering todays technologies it appears that the hardware part which realizes the data conversion at the transmitter and receiver can have a severe impact on both.

## 1.2 Data Conversion Bottleneck

One of the key enablers for the advancements of wireless communications has been digital signal processing. Digital signal processing provides a high reliability and robustness towards hardware variations, but also better means for reconfigurability and scalability, and easier ways for implementing complex systems, as compared to analog signal processing. The transmission channel of a wireless communications system remains, however, always analog. This requires to translate the digital signals, that are carrying the data, to the analog domain at the transmitter and back to the digital domain at the receiver. This is referred to as data conversion. The data conversion is in both cases determined by a resolution in time, which corresponds to the sampling rate of the digital signals, and a quantization resolution which follows from the number of amplitudes that are available to generate or approximate the analog signal.

For the design of communications transceivers that support very large bandwidths and/or which are constrained to consume very little energy, the data conversion turns out to be a major bottleneck with todays integration technologies. That is, conventional system architectures that rely on high quantization resolution at the transmitter and receiver cannot be implemented or will be subject to a performance loss due to limitations of the data conversion. At large sampling rates, which are required to support large bandwidths, technological limits restrict the quantization resolution of the data conversion. Furthermore, the larger the quantization resolution is the higher is the power dissipation of the data conversion. This can be crucial even for smaller sampling rates when targeting at lowest energy consumption.

The data conversion bottleneck can be tackled in two ways: One solution is to further improve the available integration technologies, e.g., by technology scaling. This will always involve substantial costs and may also delay the realization of emerging applications. Despite that, it will also call for alternative solutions once fundamental technological bounds are reached. The second solution is the design of system architectures that cope with constraints on the data conversion, i.e., with coarse quantization at the transmitter and receiver. Such architectures may differ from conventional system designs and require parts of the digital signal processing to be moved to the analog domain. A practical example for the latter is the 60 GHz system that has been designed for high-speed wireless point-to-point links and verified with a hardware demonstrator in the research project EASY-A (http://www.easy-a.de). The system is restricted to 1-bit data conversion and requires a frequency synchronization in the analog receiver frontend to achieve date rates of multiple Gbps. A description of the system is given in Appendix A, pp. 183. The developed demonstrator shows that it is possible to cope with limited data conversion, but an important question remains: What is an optimal system design with limited data conversion to satisfy the ever increasing demands of wireless communications.

Finding an answer to this question necessitates a theoretical characterization of the system performance under the constraints of limited data conversion. The theoretical maximum of the system performance can serve as a valuable benchmark for the development of system concepts and corresponding design paradigms. The performance metric to be considered for this purpose is the maximum data rate that can be achieved. It can be assessed with an information-theoretic system characterization, which is the main objective of this thesis. For selected cases, the thesis shows that it is even possible to derive an analytical descriptions of optimal system designs. This is, e.g., the case when the quantization resolution at the receiver is as low as 1 bit. It is also shown that this minimum resolution is very reasonable from different perspectives, including the requirement for maximum energy-efficiency.

## 1.3 Outline of the Thesis

This thesis studies the maximum data rate of wireless communications systems that are limited by the data conversion at the transmitter and receiver. The limitations reflect in a coarse quantization of the transmitted and received signals, where the quantization resolution can be as low as 1 bit. The investigations are based on an information-theoretic analysis for different types of wireless transmission channels to obtain analytical and numerical results for the maximum data rate. This includes a derivation and computation of the channel capacity, which is different and more complicated as compared to the case without quantization. Furthermore, system design requirements to achieve the maximum data rate are discussed and evaluated from a practical perspective. These requirements range from an optimized calibration of the data conversion up to the design of optimal transmission schemes. For certain channel types, such as time-dispersive channels, it turns out that optimal transmission schemes are difficult to derive. As a solution for practical system designs, sub-optimal schemes with linear channel (pre-)equalization that incorporate the data conversion at the transmitter and receiver are derived. To emphasize the need for these investigations, the technological limitations of state-of-the-art data converters and bounds on future improvements are discussed, as well. The latter includes an analysis of fundamental physical limits to the representation of digital signals. The findings on the power dissipation of data converters are applied to the information-theoretic results to identify system designs that ensure an energy-efficient data conversion at a target data rate.

The thesis is structured as follows:

- Chapter 2 provides the theoretical foundations for analyzing wireless data transmission with coarse quantization from an information-theoretic perspective. It starts with a classification of different signal types and provides a mathematical description of data conversion. A generic model for wireless communications systems is derived, which is considered throughout the thesis. The mutual information and the channel capacity are introduced as information-theoretic metrics, and possible ways for their computation are outlined.
- Chapter 3 starts with a review of common data conversion architectures and their technological limitations. The minimum power dissipation of data converters and ultimate physical limits to the representation of digital signals are discussed. Existing work is extended by considering these limitations from a pure information-theoretic perspective. The findings motivate system designs with large bandwidth but low quantization resolution to satisfy the emerging requirements on data rate and energy-efficiency.
- Chapter 4 discusses different concepts to assess and optimize the quality of quantized signals in communications transceivers. The quantization is considered from an amplitude distortion perspective, which is most common, and from an information-theoretic perspective. Optimized quantization characteristics are derived and compared for the two cases of minimum amplitude distortion and maximum mutual information. This is done for signals which are not affected by any other distortion and for distorted signals that occur in communication

systems. The information-theoretic investigations in this chapter extend previous work by considering complex-valued communications signals that can be subject to arbitrary phase offsets and by providing a geometric interpretation of the optimized quantization characteristics. Numerical examples are shown to illustrate that the quantization resolution can be kept conveniently small with the optimization while maintaining the system performance.

- Chapter 5 addresses the fundamental question of what an optimal system configuration would be to maximize the data rate with coarse quantization at the receiver. The chapter derives and analyses the capacity and respective transmit schemes for different types of wireless channels with quantization at the receiver. For additive white Gaussian noise channels, the capacity and respective transmit schemes are obtained analytically and illustrated by numerical examples. Existing work is extended by considering complex-valued signals and by taking into account coarse quantization at the transmitter, too. The power dissipation of the data conversion is incorporated in the analysis to discuss energy-efficient system designs. For time-dispersive channels, lower bounds of the channel capacity are derived, because the true capacity is difficult to calculate. Finally, frequency-flat fading channels are considered for the particular case of 1-bit quantization. The ergodic channel capacity, the optimal outage behavior and the respective transmit schemes are analytically derived for these channels.
- Chapter 6 analyzes the prospects and constraints of 1-bit quantization with oversampling at the receiver. For additive white Gaussian noise channels with rectangular pulse shaping, the channel capacity and optimal transmission schemes are calculated and illustrated by numerical examples. An important observation is the effect of stochastic resonance, which maximizes the system performance at signal-to-noise ratios below infinity. Band-limited transmission channels are analyzed numerically in terms of capacity lower bounds. It is shown that intersymbol-interference due to the band-limitation can be utilized in the same way as channel noise to improve the performance. The findings of Chapter 6 can be regarded as a generalization of previous work, which has only considered corner cases, i.e., noise-free signal reception and infinitely large oversampling.
- Chapter 7 derives linear channel (pre-)equalization schemes for time-dispersive channels with coarse quantization at the transmitter and receiver. These schemes account for the distortion of the data conversion. The (pre-)equalization criterion is the minimum mean-squared-error between the transmitted and received data symbols. The derived schemes build on existing work that has focused on frequency flat multiple-antenna channels with coarse quantization. The (pre-)equalization performance is evaluated in terms of the mutual information that can be achieved. It is shown that a performance degradation due to coarse quantization can be mitigated with higher sampling rates and fractionally-spaced (pre-)equalization that builds on a system design with time-interleaved data conversion.
- Chapter 8 summarizes the main results and outlines important directions for further research to integrate the findings of this thesis into future system designs.

Each of the Chapters 3 to 7 concentrates on a specific topic. Related literature and the very particular contributions of this thesis are detailed at the beginning of each of the chapters.

As mentioned before, a brief description of the 60 GHz demonstrator that has been developed in the EASY-A project is given in Appendix A. An in-depth explanation of different ways to compute the mutual information and channel capacity under various constraints is provided in Appendix B. Appendix C contains parameter tables and selected derivations for optimized quantization characteristics which are considered in this thesis. The proofs of all theorems of this thesis are given in Appendix D.